Modeling the Local Response of Gain Media in Time-Domain

Nikita Arnold,[1] Ludmila Prokopeva,[2] and Alexander V. Kildsihev[2]

[1]Institute of Applied Physics,
Johannes Kepler University, Linz, Austria
nikita.arnold@jku.at

[2]Birck Nanotechnology Center, Department of Electrical and Computer Engineering
Purdue University, West Lafayette, IN 47907, USA
lprokop@purdue.edu
kildishev@purdue.edu

Abstract: We present a new, in-the-cloud modeling tool that we plan to stage at nanoHUB (www.nanoHUB.org). The tool provides the time-domain simulation of 4-level atomic gain system and post-processing analyses of the optical amplification process.

Keywords: Gain Media, Time-Domain, Optical Amplification

1. Introduction

This paper describes a PhotonicsGAIN-0D simulation tool, which is planned to be staged at nanoHUB (www.nanoHUB.org) and provides time-domain simulation of 4-level atomic gain system and post-processing analyses of the optical amplification process. The tool adds to the collection of our other nanophotonics tools at nanoHUB [1-6]: PhotonicsDB – the material database of optical properties of various materials, PhotonicsRT – simulates planar nanostructured lamellar photonic crystals and non-reflecting coatings, PhotonicsSHA-2D – simulates cascaded photonic or plasmonic 2D metamaterials, PhotonicsCL – simulates cylindrical transformation optics lenses, Hyperlens Layer Designer and Hyperlens Design Solver – simulate cylindrical hyperlenses. These tools deliver a cloud computing service, offering off-site simulations done through standard web browsers, with no demand for either powerful computational hardware or any additional software installations. The hosting hardware and software platforms are provided by the Network for Computational Nanotechnology (NCN) at the Birck Nanotechnology Center at Purdue University. Along with the scientific simulation services, nanoHUB's cloud computing services also include courses, software tutorials, discussion groups and Internet-based infrastructure for effective collaboration in the major areas of nanoelectronics, nanoelectromechanical systems, and their application to nano-biosystems.

The development of the PhotonicsGAIN-0D solver has been motivated by the problem of achieving loss compensation in plasmonic elements of optical metamaterials. A recent approach to this problem is to introduce organic dyes into a dielectric host of the metamaterial structure [7-17], and use light amplification based on the stimulated radiation emission from the dye-doped host, a phenomenon broadly used in laser science [18-19].

For amplification, the gain medium is first pumped optically; then, it can emit photons upon the relaxation of excited levels. The gain medium (or a dye-doped host) is formalized as a quantum mechanical system of "atoms" (here, a general term for any atoms, molecules, ions, or semiconductor structures). The pumping process excites the atoms into higher quantum-mechanical energy levels. Then, for the loss-compensation or amplification to occur, the pumping process must generate a *population inversion*, i.e. more atoms must be excited into some higher i-th quantum energy level (E_i) than there

are at some lower j-th energy level (E_j) of the lasing medium. Once the population inversion between the levels i, j is obtained, electromagnetic radiation within a certain narrow band of frequencies (near the frequency of the inverted transition $\omega_{ij} = (E_i - E_j)/\hbar$) can be coherently amplified, when going through a thick enough slab of gain medium (in laser generators, the signal goes back and forth between the mirrors, which provides additional positive feedback).

In this tool, instead of modeling full-wave pulse propagation through a gain medium, we study the local response (at a fixed spatial point) of the gain medium to a given external time-dependent electric field – we calculate the population kinetics on all energy levels (pumping process, inversion, and then relaxation) and the effective frequency domain polarizability (susceptibility). The tool helps to study, validate, and fit to the experimental data a simplified 4-level atomic model of a given gain medium.

Real gain systems may involve a large number of energy levels, but many of them can be reduced to the four-level atomic system with similar essential features and semi-quantitative behavior. For this reason we hope that the tool is helpful for different applications of gain media beyond active metamaterials, e.g., in organic dye lasers, and organic dye spectroscopy.

In sections below we list notations and acronyms used in the document and GUI of the tool, and then give a detailed description of the four-level atomic system, simulated by the tool. All the simulation examples were performed for the 4-level gain system of Rhodamine800 dye. Parameters of this system were found by fitting simulation results to the pump-probe experiment in [16], and they are set by default in the GUI of the tool.

2. 4-Level Atomic System Model

We assume that the atomic system has 4 energy levels (Fig. 1). The zero-th level is the ground level hosting the total population of the non-excited system. In our model the ground level atoms can be pumped with an external electric field to the highest level E_3. Then, under certain constraints on relaxation times (e.g., the relaxation time of 32 transition must be smaller than that of 21 and 30 transitions), the pumped system will get an inversion of levels E_2 sand E_1, between which the lasing takes place.

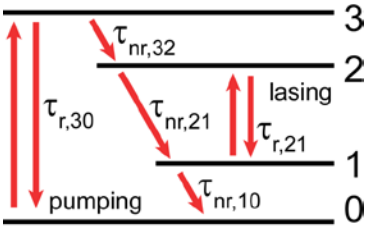

Figure 1. An energy transition diagram of the four-level atomic system.

The system relaxes exponentially, towards the Boltzmann equilibrium. We assume that initially the system is not excited – all the population is at the ground level (which is a good approximation for VIS range). Thus, if $N_i(t)$ is the relative population density function of time at level E_i, the population kinetics of the entire system shown in Fig. 1 satisfies the following system of ordinary differential equations (ODE) [14,16,19]

$$\begin{cases} N_3' = -\tau_{32}^{-1} N_3 + f_{30} \\ N_2' = -\tau_{21}^{-1} N_2 + \tau_{32}^{-1} N_3 + f_{21} \\ N_1' = -\tau_{10}^{-1} N_1 + \tau_{21}^{-1} N_2 - f_{21}, \quad t > 0. \\ N_0' = \tau_{10}^{-1} N_1 - f_{30} \\ N_0(0) = 1; N_1(0) = N_2(0) = N_3(0) = 0 \end{cases} \tag{1}$$

The first right hand side column defines the exponential relaxation of the upper level to the lower level with the total decay time τ_{ij} for each ij-transition. The second column is the inflow to the lower level produced by the relaxation of the upper level. The third column accounts for the radiative transitions between the levels stimulated by the external electric field. The total population $N_0(t) + N_1(t) + N_2(t) + N_3(t) = 1$ is conserved. In general, the total decay rate of each transition includes a radiative and a non-radiative part $\tau_{ij}^{-1} = \tau_{\mathrm{r},ij}^{-1} + \tau_{\mathrm{nr},ij}^{-1}$. Here we assume that only transitions 30 and 21 have a radiative part, and the non-radiative part of transition 30 is neglected (Fig. 1). The radiative lifetime of the pumping transition $\tau_{\mathrm{r},30}$ is usually large; it contributes to the driving terms f_{ij} but is neglected as a relaxation term in population equations (1), since $\tau_{\mathrm{r},30} \gg \tau_{32}$.

The driving terms f_{ij} stimulated by the external electric field $E(t)$ are given by [14,16]

$$f_{ij} = \eta_{ij} E\left[P'_{ij} + \tfrac{1}{2}\Gamma_{ij} P_{ij}\right], \quad ij \in \{21, 30\}, \tag{2}$$

where $\eta_{ij} = \varepsilon_0 / (N_{tot}\hbar\omega_{ij})$; ω_{ij}, Γ_{ij}, P_{ij} are the Lorentzian frequency, damping constant, and polarization of the transition. The physical origin of driving terms (2) lies in the energy exchange between the atomic dipoles and the external field, recalculated into the number of photons [19]. In the GUI we allow for setting wavelength rather than the frequency, so that $\lambda_{ij} = 2\pi c / \omega_{ij}$.

Each polarization $P_{ij}(t)$ satisfies the Lorentz ODE, reflecting decay and dephasing of the individual atomic dipoles [19]

$$P''_{ij} + \Gamma_{ij} P'_{ij} + \omega_{ij}^2 P_{ij} = \kappa_{ij}\left[N_j - N_i\right]\left[E + \nu_{ij} E'\right], \; ij \in \{30, 21\} \tag{3}$$

with an additional term ($\nu_{ij} E'$) defining a phase-shift in response, and the entire excitation term being proportional to the difference in populations. Here, the coupling coefficients are: $\kappa_{ij} = 6\pi N_{tot} c^3 / (\tau_{\mathrm{r},ij}\omega_{ij}^2\sqrt{\varepsilon_{\mathrm{h}}})$, $\nu_{ij} = 2\sin\phi_{ij} / (\Gamma_{ij}\sin\phi_{ij} - \sqrt{4\omega_{ij}^2 - \Gamma_{ij}^2}\cos\phi_{ij})$, and ε_h is the permittivity of the host media. If the phase ϕ_{ij} is zero, then $\nu_{ij} = 0$, and we get the classical Lorentz oscillator model. By adding a nonzero phase ϕ_{ij} we add non-symmetry to the Lorentzian lineshape in frequency domain. In the time domain this corresponds to the same damping oscillator but with a shift, so that in the assumption of constant population difference $N_{ij} = N_i - N_j$ we have $\chi_{ij}(t) = A_{ij} e^{-\Gamma_{ij} t}\sin(\omega_{ij} t - \phi_{ij})$, $A_{ij} = \kappa_{ij} N_{ij}\left(\omega_{ij}^2 - \Gamma_{ij}^2/4\right)^{-1/2}$. The susceptibility χ_{ij} is defined in frequency domain as $\chi_{ij}(\omega) = \hat{P}_{ij}(\omega) / \hat{E}(\omega)$. This expression for κ_{ij} corresponds to dipoles fully aligned with the exciting field $\mathbf{E}(t)$. For randomly oriented dipoles this coefficient is three times smaller.

3. External Field and Pump-probing

In the absence of the external electric field, the polarizations $P_{ij}(t)$ and driving terms $f_{ij}(t)$ are equal to zero, and the system remains in the initial equilibrium non-excited state.

To achieve the population inversion and gain in the lasing transition 21, the pumping pulse with high enough external field must be applied to a system. Its spectrum is usually in a close proximity of a frequency ω_{30}. The polarization P_{30}, and therefore the driving term f_{30}, are proportional to the external field, but also to the population difference $(N_0 - N_3)$ at a given time, see eq. (1-3). Therefore the population difference determines the strength and the direction of the induced flow of population f_{30} between the levels 3 and 0. Positive f_{30} means transition to higher energy level and is accompanied with

the absorption of energy, while negative f_{30} means population relaxation to ground level and is followed by emission. Typically, because of fast non-radiative relaxations and slow transition 30, population difference $(N_0 - N_3)$ remains positive, or may tend to zero in case of long high intensity pulses. However, shorter pumping pulses with high external electric field values may lead to $N_3 > N_0$. In this situation the transition 30 will coherently absorb and re-emit photons in a cycle for some time (Rabi type oscillations [19] of populations N_0 and N_3), see fig. 2c for an example.

After the gain system has been pumped, the relaxation time of the whole system is determined by the total lifetime of the lasing transition, which is usually the slowest lifetime in the system. E.g., for Rh800 [16] the total lifetime of the lasing transition is about 3 ns, the pumping radiative lifetime is roughly 30 ns, and non-radiative transitions 32 and 10 are much faster – with less than 0.3 ps lifetimes. Before the inversion of the lasing transition relaxes, we set a probing pulse to estimate the amplification of the gain system (typical delay between pump and probe for Rhodamine800 experiment [16] was 50 ps). The probe pulse is usually several orders weaker than the pump pulse and its spectrum is usually in the vicinity of the lasing frequency ω_{21}. As opposed to pump transition, the sign of the population difference $(N_1 - N_2)$ is negative for a pumped system and zero otherwise. Maximum inversion provides maximum emission; if inversion is insufficient (and absorbing transition 30 is not saturated) the probe pulse will be entirely absorbed by the pumping transition 30, see e.g., fig 3a

To estimate amplification/absorption of the pump and probe pulses we calculate efficient susceptibility $\chi_{ij}(\omega)$ for each pump and probe part of the external field and polarizations. The susceptibility is defined in frequency domain as $\chi_{ij}(\omega) = \mathrm{FT}\left(P_{ij}\big|_{[t_1,t_2]}\right) / \mathrm{FT}\left(E\big|_{[t_1,t_2]}\right)$, where FT means the Fourier Transform of a time domain function, and $[t_1,t_2]$ is the time range corresponding to pump or probe pulse. The analytical estimate of the susceptibility can be made from eq. (3) by assuming $N_0 - N_3 = 1$ (maximum absorption) and $N_1 - N_2 = -1$ (maximum emission)

$$\chi_{ij}(\omega) \approx \frac{\kappa_{ij} n_{ij}\left[1 - \iota\omega\nu_{ij}\right]}{-\omega^2 - \iota\omega\Gamma_{ij} + \omega_{ij}^2} \quad ij \in \{30,21\},\ n_{30} = 1,\ n_{21} = -1,\ ij \in \{30,21\}. \tag{4}$$

This ideal analytical absorption can be reached in practice for transition 30 in unsaturated system. However, the inversion value $N_2 - N_1$ that can be reached by pumping process is usually far away from 100% (about 40% for Rhodamine800 [16]), and the practical emission rate is typically below half its analytical estimation.

In the GUI we assume both pump and probe pulses to be Gaussian

$$E(t) = \sum_{\mathrm{i=pump,\ probe}} A_i \exp\{-(t - t_{0,i})^2 \,/\, 2\sigma_i^2\} \sin\omega_i t \quad (t_{0,\mathrm{pump}} < t_{0,\mathrm{probe}}). \tag{5}$$

4. Simulation Example of RH800

The parameters of the four-level gain system of Rhodamine800 dye in a solid host [16] are set by default in the GUI of the tool. We first vary the parameters of the pumping pulse, which can be shorter or longer, but its power should be high enough to invert the lasing transition. In Figure 1 we show an example of the pumping process for a gain system [16] using 100-fs (FWHM of the intensity, i.e., $\mathrm{FWHM}=\sigma 2\sqrt{\log 2}$) and 2-ps pumping pulses with: (a) low power, which only slightly affects the populations, (b) medium power, sufficient to get appreciable inversion of 21 transition, (c) high power which shows the behavior of the saturated system. The intensities for 2-ps pulse are scaled down to preserve the same power level as in cases (a)-(c) for the shorter, 100-fs pulse. This simulation helps to estimate the power required to achieve inversion and to compare inversion rates for short and long pulses in a given gain system, see Fig. 2. The shorter pulse results in slightly larger population inversion of the

lasing transition 21 (44% versus 39%). As discussed in the previous section, for short and intensive pump pulse (100-fs, 3e9 V/m) Rabi oscillations occur in this gain system for the pumping transition 30.

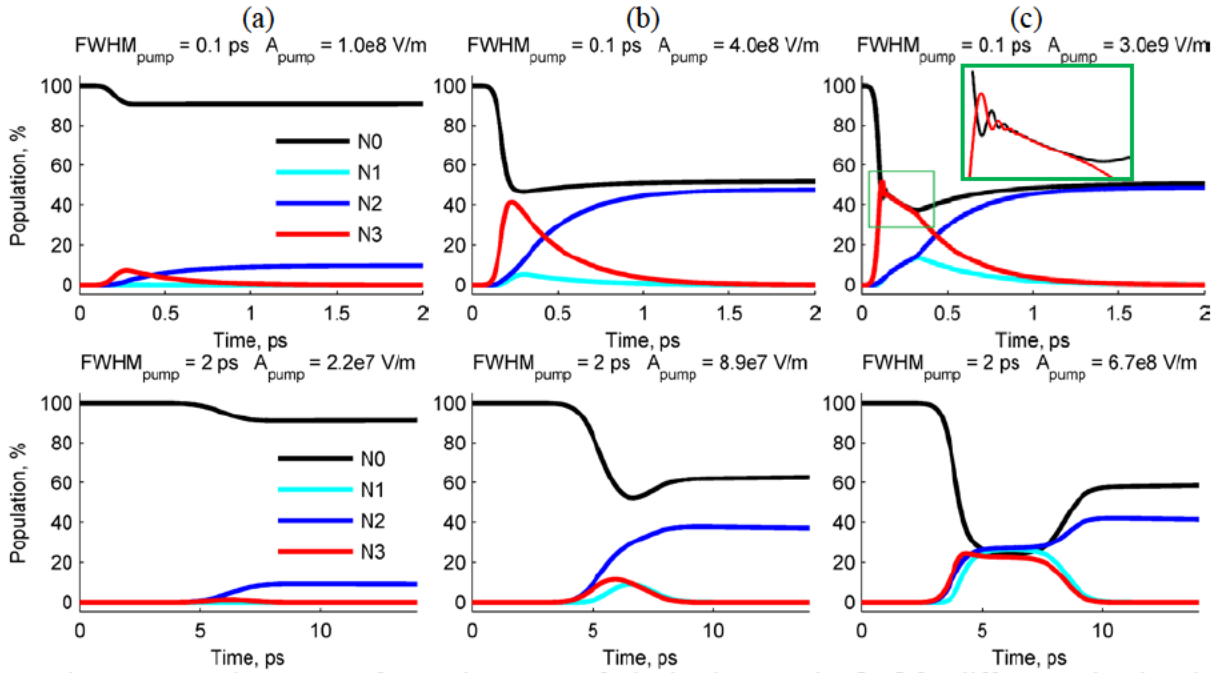

Figure 2. Pumping process for a gain system of Rhodamine 800 dye [16] for different pulse durations and intensities. Upper panel $\sigma_{pump} = 100$ fs pulse, (a) $A_{pump} = 10^8$ (b) $A_{pump} = 4\times10^8$ (c) $A_{pump} = 3\times10^9$. Lower panel $\sigma_{pump} = 2$ ps pulse, (a) $A_{pump} = 2.2\times10^7$ (b) $A_{pump} = 8.9\times10^7$ (c) $A_{pump} = 6.7\times10^8$.

Once the parameters of the pumping pulse are set, the amplification of the probe signal can be examined by plotting the imaginary part of the frequency domain susceptibility. In Fig. 3 we plot the imaginary part of χ_{30}, χ_{21} susceptibilities and the resulting sum $\chi_{30} + \chi_{21}$ for the probe pulse (FWHM = 5 fs, 1e6 V/m) delayed by 15 ps from the pump and for three variants of the pumping process (Fig. 2abc). Dotted color-matched lines in Fig. 3 are analytical estimates of susceptibilities (Eq. (4)). As predicted in the previous section, if the gain system is insufficiently pumped (Fig. 3a) then absorption is close to its analytical estimation and absorption $\mathrm{Im}\,\chi_{30} > 0$ dominates over the small emission $\mathrm{Im}\,\chi_{21} < 0$, so that the resulting response $\chi_{30} + \chi_{21}$ has absorption in the entire range. As the 30 absorber saturates (Fig. 3bc), the absorption lineshape decreases below its analytical estimation. At the same time, the emission becomes sufficiently stronger than in case (a), so that the resulting response has emission in the entire shown range. The deviation of the emission from its analytical estimate (4) is explained by incomplete populations inversion of transition 21 see Fig. 2c. The difference between Fig. 3b and Fig. 3c is insignificant with the latter having a slightly larger emission rate and lower absorption peak.

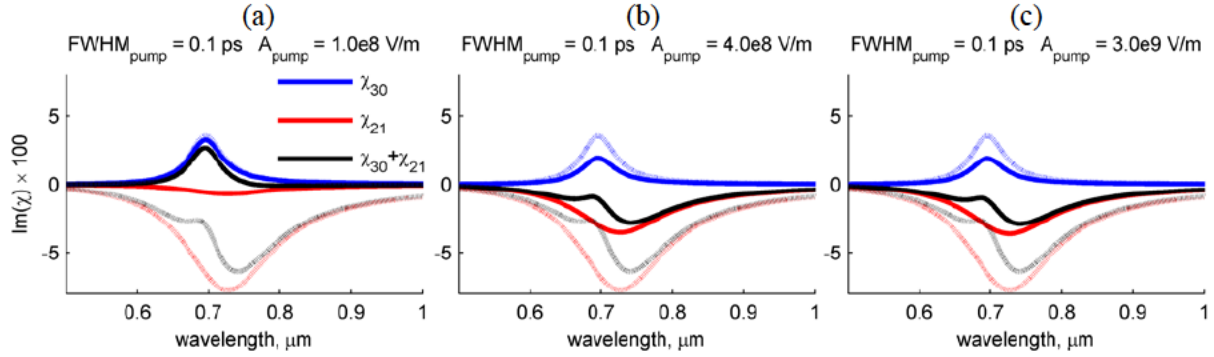

Figure 3. Imaginary part of frequency domain susceptibility of the probe pulse for three pumping processes (see fig.2). The dotted lines show analytical estimates, as in eq. (4). The resulting sum (black line) demonstrates emission for cases (b-c), while in case (a) the probe pulse is absorbed by pumping transition 30.

5. Conclusion

We have presented a new simulation tool PhotonicsGAIN-0D which provides time-domain simulations of active media described by a four-level atomic system and is freely available at nanoHUB.org. AVK and LJP gratefully cite the support from the AFRL Materials & Manufacturing Directorate Applied Metamaterials Program. NA acknowledges funding from the ERC Starting Grant 257158 “Active NP”.

References

[1] X. Ni et al., “PhotonicsDB: Optical Constants,” *NanoHUB.org*, http://nanohub.org/resources/photonicscdb, 2008.
[2] S. Ishii, et al., "PhotonicsRT: Wave Propagation in Multilayer Structures,” *NanoHUB.org*, http://nanohub.org/resources/photonicscrt, 2008.
[3] X. Ni et al., “PhotonicsSHA-2D: Modeling of Single-Period Multilayer Optical Gratings and Metamaterials,” *NanoHUB.org*, http://nanohub.org/resources/sha2d, 2009.
[4] M. Swanson et al., "Hyperlens Layer Designer,” http://nanohub.org/resources/hypiedesigner, *NanoHUB.org*, 2008.
[5] M. Swanson et al., “Hyperlens Design Solver,” *NanoHUB.org*, http://nanohub.org/resources/hypiesolver, 2008.
[6] X. Ni et al. “PhotonicsCL: Photonic Cylindrical Multilayer Lenses,” *NanoHUB.org*, http://nanohub.org/resources/photonicscl, 2011.
[7] M. I. Stockman “The Spaser as a Nanoscale Quantum Generator and Ultrafast Amplifier,” *J. Opt.*, vol. 12, pp. 024004, 2010.
[8] M. Noginov et al., “Enhancement of Surface Plasmons in an Ag Aggregate by Optical Gain in a Dielectric Medium,” *Opt. Lett.*, vol. 31, pp. 3022-3024, 2006.
[9] N. I. Zheludev et al., “Lasing Spaser,” *Nat. Photonics*, vol. 2, pp. 351-354, 2008.
[10] E. Plum et al., “Towards the Lasing Spaser: Controlling Metamaterial Optical Response with Semiconductor Quantum Dots,” *Opt. Express*, vol. 17, pp. 8548-8551, 2009.
[11] A.K. Sarychev and G. Tartakovsky, “Magnetic Plasmonic Metamaterials in Actively Pumped Host Medium and Plasmonic Nanolaser,” *Phys. Rev. B*, vol. 75, pp. 085436, 2007.
[12] S. M. Xiao et al., “Loss-free and Active Optical Negative-Index Metamaterials,” *Nature*, vol. 466, pp. 735-U6, 2010.
[13] A. Fang, “Self-consistent Calculation of Metamaterial with Gain,” *Phys. Rev. B*, vol. 79, pp. 241104, 2009.
[14] S. Wuestner et al., “Gain and Plasmon Dynamics in Active Negative-Index Metamaterials,” *Phil. Trans. R. Soc. A*, vol. 369, pp. 3525-3550, 2011.
[15] T. A. Klar et al., “Negative-Index Metamaterials: Going Optical, *IEEE J. Sel. Top. Quantum Electron.*,” vol. 12, no. 6, pp. 1106-1115, 2006.
[16] J. Trieschmann et al., “Experimental Retrieval of the Kinetic Parameters of a Dye in a Solid Film,” *Opt. Express*, vol. 19, pp. 18253-18259, 2011.
[17] L. J. Prokopeva et al., “Numerical Modeling of Active Plasmonic Metamaterials,” *Proc. SPIE*, vol. 8172, pp. 81720B, 2011.
[18] B. E. A. Saleh and M. C. Teich, *Fundamentals of photonics*, Wiley-Interscience, New York, 2007.
[19] A. E. Siegman, *Lasers*, University Science Books, Sausalito, CA, 1986.